Electronic Supplementary Material (ESI) for ChemComm.

Supplementary Information

Understanding Electrochemical Cation Insertion into Prussian Blue from Electrode Deformation and Mass Changes

Saeed Saeed[1], Shelby Boyd[1], Wan-Yu Tsai[2], Ruocun Wang[1], Nina Balke[3], and Veronica Augustyn[1*]

[1] Department of Materials Science and Engineering, North Carolina State University, Raleigh, NC 27606

[2] Chemical Science Division, Oak Ridge National Laboratory, Oak Ridge, Tennessee 37830

[3] Center for Nanophase Materials Sciences, Oak Ridge National Laboratory, Oak Ridge, Tennessee 37830

[*] corresponding author, email: vaugust@ncsu.edu

Methods

Materials Synthesis: Prussian blue thin films were synthesized via electrodeposition.[1] The electrodeposition solution consisted of 5 mL of 0.05 M HCl (Fisher Chemical, Certified ACS Plus), 10 mL of 0.05 M $K_3[Fe(CN)_6]$ (Sigma-Aldrich, Certified ACS Crystalline), and 10 mL of 0.05 M $FeCl_3$ (Alfa Aesar, 98%) which was added to a 50 mL glass three-neck flask containing a magnetic stir bar. Chronopotentiometry was performed with a potentiostat (Pine Research WaveNow) onto a glassy carbon disk (HTW-Germany; d = 10 mm, thickness = 1 mm, both sides lapped, one side diamond polished) as the working electrode, Ag/AgCl in 4 M KCl (Pine Instruments) as the reference electrode, and a platinum wire (Alfa Aesar, 99.997%) as the counter electrode. The Prussian blue was deposited on the glassy carbon at a current of 40 $\mu A/cm^2$ for 1 minute. After deposition, the film was rinsed with DI water and placed in a 60°C oven overnight. The typical film mass via quartz crystal microbalance (QCM) was ~ 0.14 mg/cm^2.

Physical Characterization: Scanning electron microscopy (SEM) and energy dispersive X-ray spectroscopy (EDS) were conducted using an FEI Verios 460L. Raman spectroscopy was performed using a Witec Alpha 300 Confocal Microscope with a 532 nm Nd: YAG laser and a 100x objective lens. The laser wavelength was first calibrated by adjusting the strong peak of a Si wafer to 520 cm^{-1}. X-ray diffraction (XRD) was performed on a PANalytical Empyrean using Bragg-Brentano geometry and Cu-Kα radiation.

Electrochemical Characterization: Three-electrode cells were prepared in glass three-neck round bottom flasks with the electrodeposited Prussian blue as the working electrode, Ag/AgCl as the reference electrode, and a Pt wire counter electrode (as noted above). The electrolytes used were 0.5 M K_2SO_4 (Fischer Chemical, Certified ACS), 0.5 M Na_2SO_4 (Sigma-Aldrich, ACS reagent, ≥99.0%), and 0.5 M Li_2SO_4 (Sigma-Aldrich, ≥ 98.5%). Cyclic voltammetry was performed between a potential range of -0.2 - 0.6 V vs. Ag/AgCl at scan rates from 10 – 200 mV/s using a Bio-Logic MPG-2 potentiostat. This range of scan rates was selected to correlate with AFM

results, because the drift of the AFM tip becomes non-negligible during *operando* dilatometry measurements at slower rates.

Electrochemical Quartz Crystal Microbalance: EQCM measurements were performed with a QCM200 quartz crystal microbalance digital controller and a QCM25 5MHz crystal oscillator (Stanford Research Systems, Inc.). Prussian blue was deposited onto a gold-plated AT-cut quartz crystal with a fundamental frequency of 5MHz and a working electrode area of 1.419cm^2 (Phillip Technologies). Before cyclic voltammetry, the resonant frequency of the quartz crystal was allowed to equilibrate for at least 30 minutes. Cyclic voltammetry was performed in 0.5 M K_2SO_4 between -0.2 and 0.6 V vs. Ag/AgCl from 10 – 200 mV/s. 10 cycles were collected at each scan rate using a 200 Hz/V conversion factor for the output signal on the QCM controller. To quantitatively determine the mass gained and lost during cycling from the resonant frequency, the silver deposition method was used to calculate the calibration factor (24.1 Hz/μg).[2,3] The measured data was analyzed using a Matlab program that took smoothed the raw data with a Savitzky-Golay filter, did a baseline subtraction, and calculated the average and derivative of the mass change across all 10 cycles. The program was based on that described by Wang et al.[4]

***Operando* AFM:** *Operando* AFM dilatometry measurements were conducted using a commercial in situ electrochemical AFM cell and MFP-3D atomic force microscope (both from Asylum Research, USA) with ElectriMulti75-G (BudgetSensors) AFM cantilevers (nominal spring constant = 3 N/m). Electrode deformation measurements were obtained using two methods. For deformation measurement on individual spots, a contact mode with constant force feedback was used. For the 5 × 5 point grid map, the AFM cantilever performed a force−distance curve at each spot and triggered the potentiostat to run cyclic voltammetry at 100 mV/s for 20 cycles during the contact part of the force−distance curve. After the cyclic voltammetry was finished, the cantilever withdrew and moved to the next spot. The above procedure was repeated for all 25 points on the grid. The electrode deformation was recorded by the deflection of the cantilever. Electrochemical

characterization was performed with a Bio-Logic SP-300 potentiostat (Bio-Logic, USA) in a three-electrode configuration with Ag/AgCl reference and glassy carbon counter electrodes in 0.5 M K_2SO_4 as the electrolyte. The EC-Lab software (Bio-Logic) recorded the time, potential of the working electrode, current, and deformation signal from the microscope in units of volts. The conversion of the deformation signal to the unit of length was obtained by taking the slope of the retraction part of the force−distance curve. The measured dilatometry data was analyzed using a Matlab program that took the average and derivative of the deformation. Raw data was smoothed with a Savitzky-Golay filter. Further details on the program are described by Wang et al.[4]

Supplementary Figures and Table

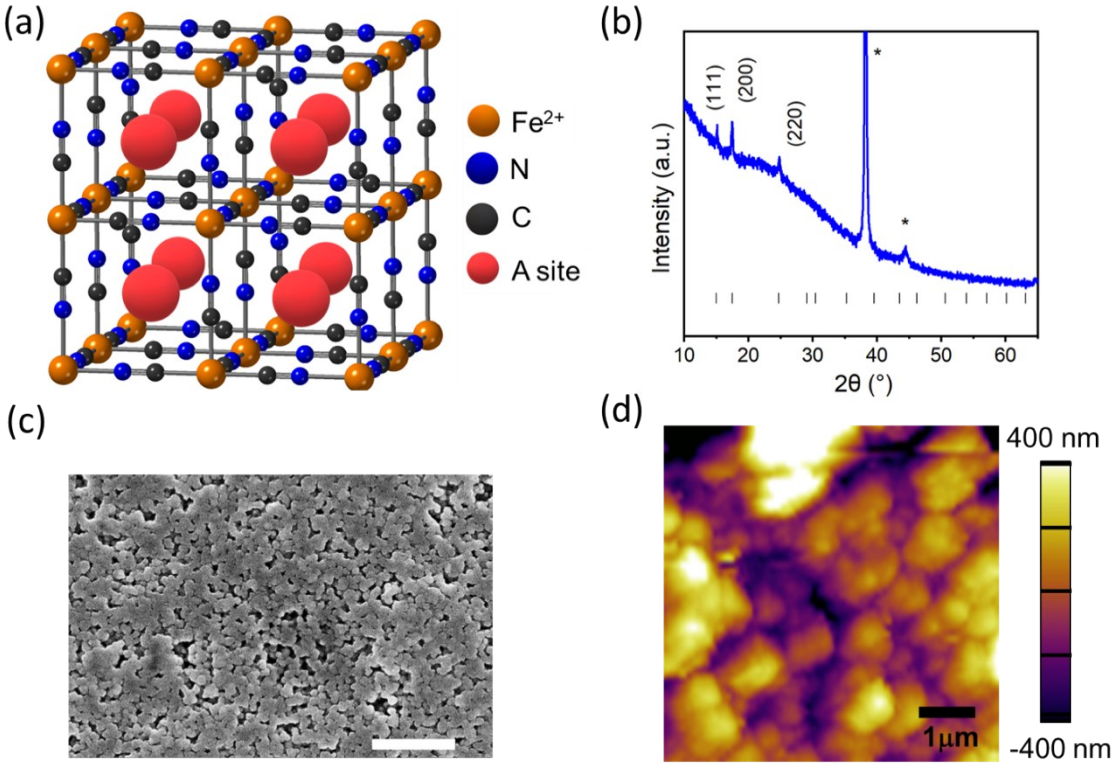

Figure S1 Structure and morphology of electrodeposited Prussian blue films. (a) Prototypical, vacancy-free cubic structure of Prussian blue with occupied alkali cation insertion sites ("A site"), (b) XRD of a typical film on gold-coated glass (reference = PDF #00-052-1907; * = gold substrate) shows that the films exhibit the expected cubic structure of Prussian blue. Minor peaks are not observed due to the large substrate background. The XRD results indicate no preferential orientation, which agrees with the lack of obvious faceting in the electrodeposited grains. (c) SEM image of the film on a glassy carbon substrate (scale bar = 500 nm) showing interconnected spherical grains ~ 62 ± 6 nm in diameter. (d) AFM tomography in 0.5 M K_2SO_4 shows larger grain sizes and a rougher electrode surface (> 800 nm) as compared to the SEM results. The differences might originate from heterogeneity of the electrodeposited film, morphology changes upon electrolyte immersion, and tip convolution effects.

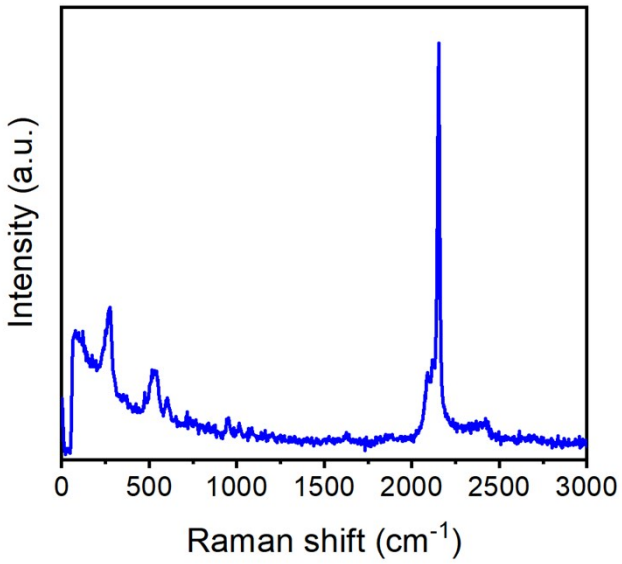

Figure S2 Raman spectrum of the electrodeposited Prussian blue film. The peaks at 2153 and 2090 correspond to, respectively, the A_{1g} and E_g mode of the CN stretch (νCN).[5,6] The peaks at lower wavenumbers have been assigned to various stretching and bending modes, though these are less well-defined: ν(Fe-C) between 350 – 600 cm^{-1}, δ(Fe-C-N) between 350 – 500 cm^{-1}, and δ(C-Fe-C) between 60 – 130 cm^{-1}.[7 7]

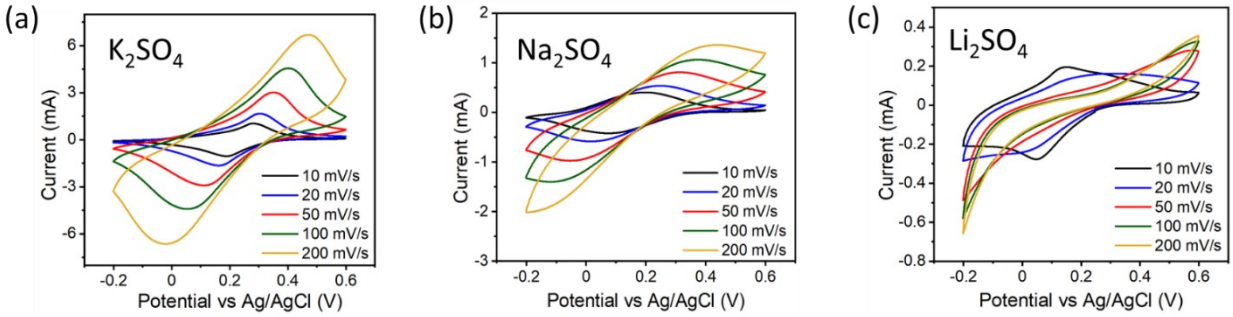

Figure S3 Cyclic voltammetry of electrodeposited Prussian blue films in aqueous electrolytes. a) 0.5 M K_2SO_4, b) 0.5 M Na_2SO_4, and c) 0.5 M Li_2SO_4 at scan rates 10 – 200 mV/s.

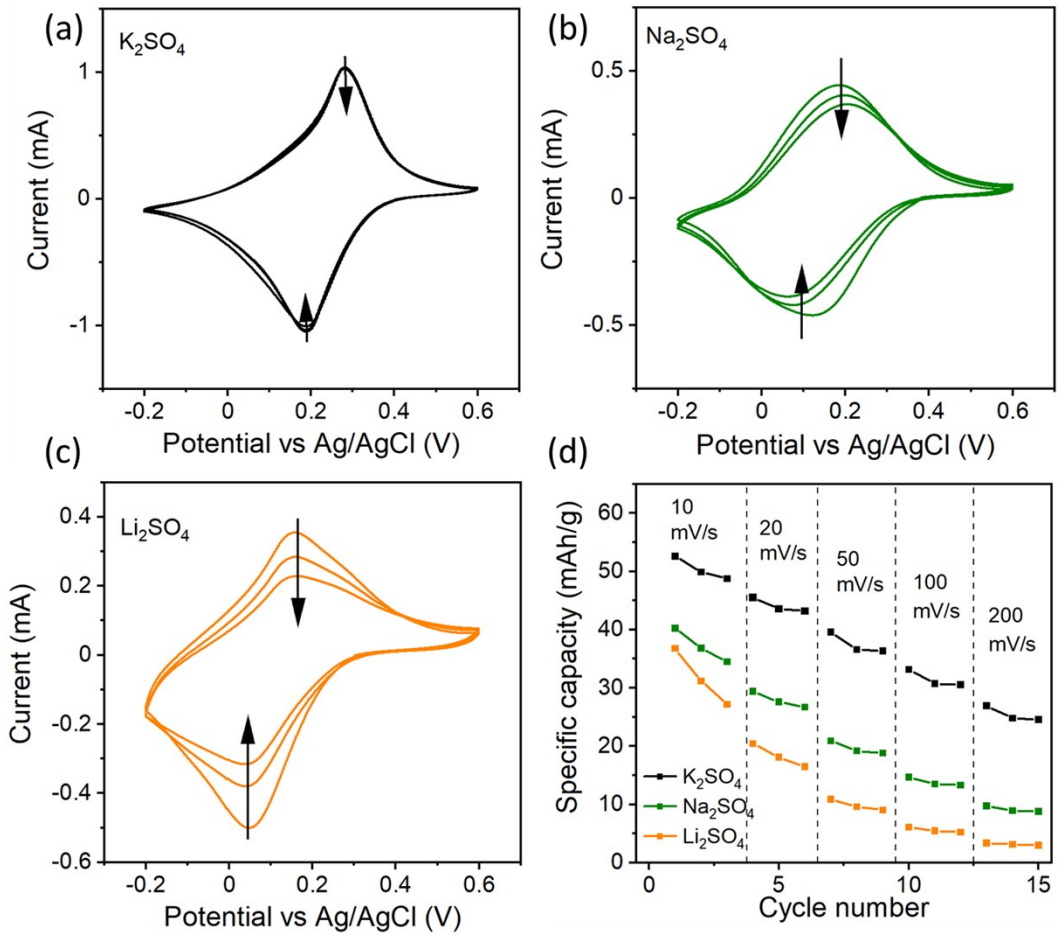

Figure S4 Cycling stability of electrodeposited Prussian blue films in aqueous electrolytes. a) 0.5 M K_2SO_4, b) 0.5 M Na_2SO_4, and c) 0.5 M Li_2SO_4 at 10 mV/s. Black arrows indicate the direction of current change from cycle 1 to cycle 3. d) Cathodic capacity as a function of cycle number and sweep rate in the three electrolytes.

Table S1 Comparison of the ionic radii (r_{ion}), hydrated radii (r_{hyd}), and associated hydration free energies of selected alkali cations.

Cation	r_{ion} (Å)[8]	r_{hyd} (Å)[9]	ΔG_{hyd} (kJ/mol)[10]
Li^+	0.69	2.37	-475
Na^+	1.02	1.83	-369
K^+	1.37	1.38	-295

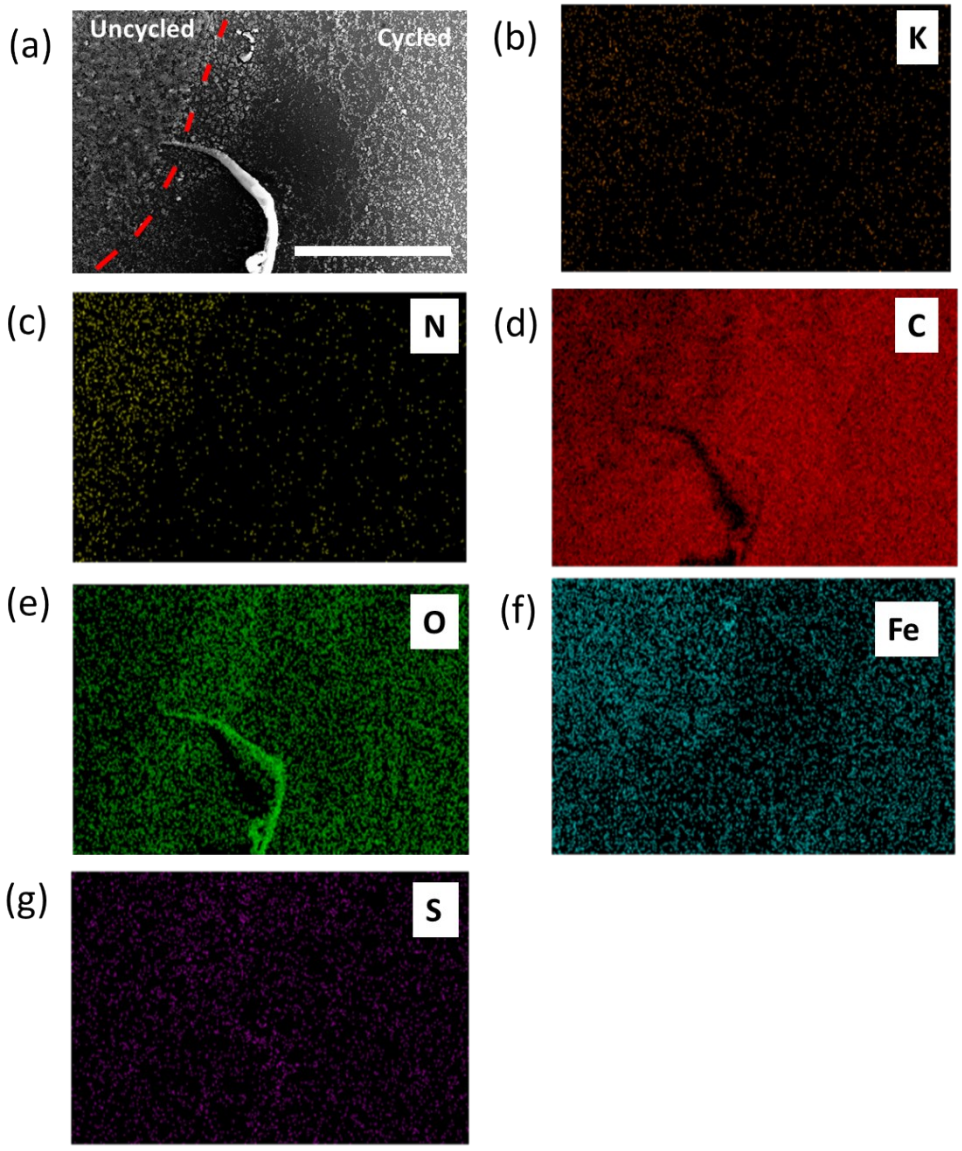

Figure S5 a) SEM image of a Prussian blue thin film electrodeposited on glassy carbon at the interface of a cycled and uncycled region in a Li_2SO_4 electrolyte. EDS maps of the same region of b) potassium, c) nitrogen, d) carbon. e) oxygen, f) iron, and g) sulfur. Scale bar = 1 μm. The results show less potassium, iron, and nitrogen in the cycled region as compared to the uncycled region, indicating loss of active material.

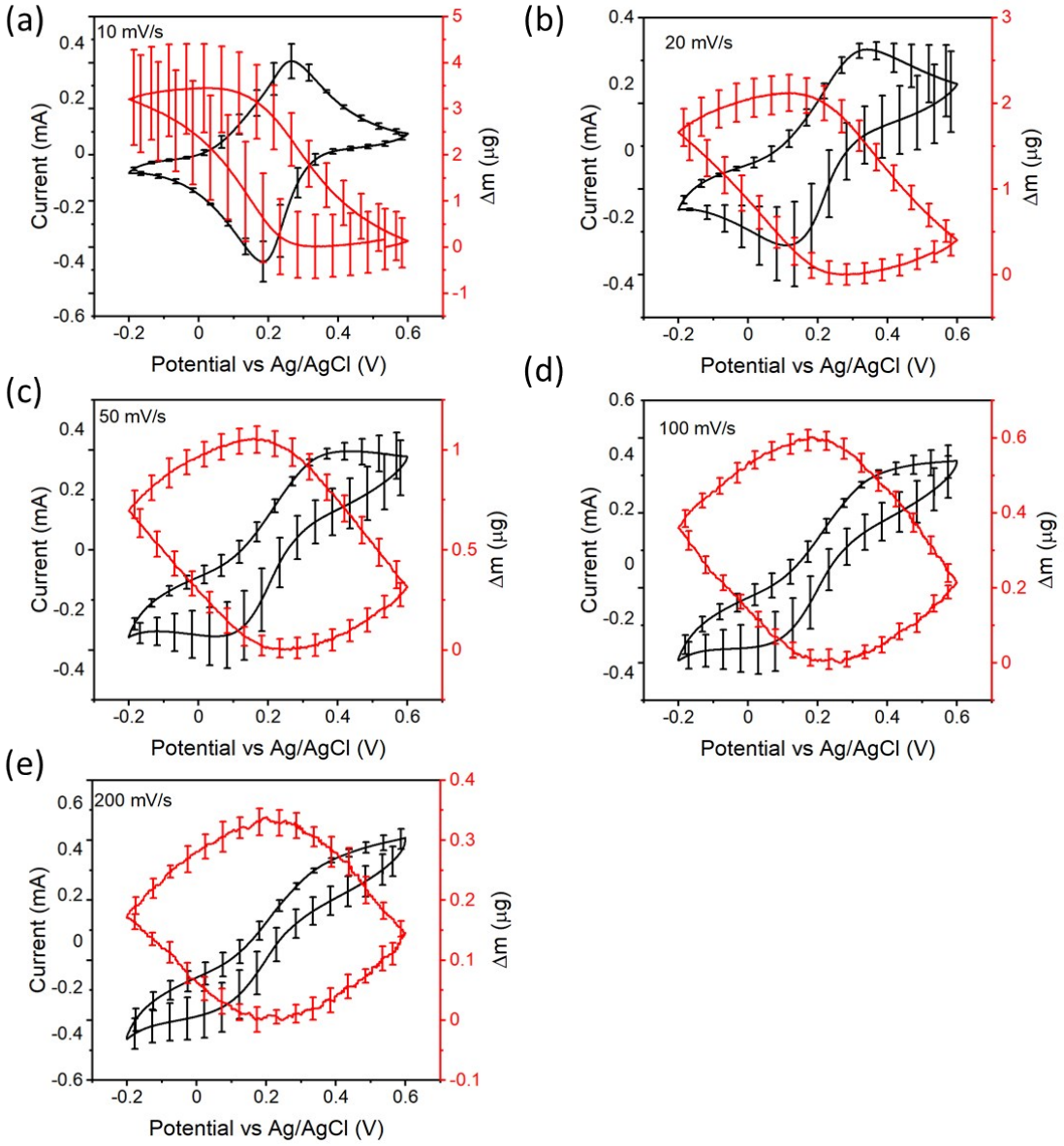

Figure S6 Mass change (from EQCM) vs. potential overlaid with CVs of a Prussian blue thin film cycled in 0.5 M K_2SO_4 for a) 10 mV/s, b) 20 mV/s, c) 50 mV/s, d) 100 mV/s, and e) 200 mV/s. Error bars indicate the standard deviation of the current and mass change at specific potentials for 10 cycles.

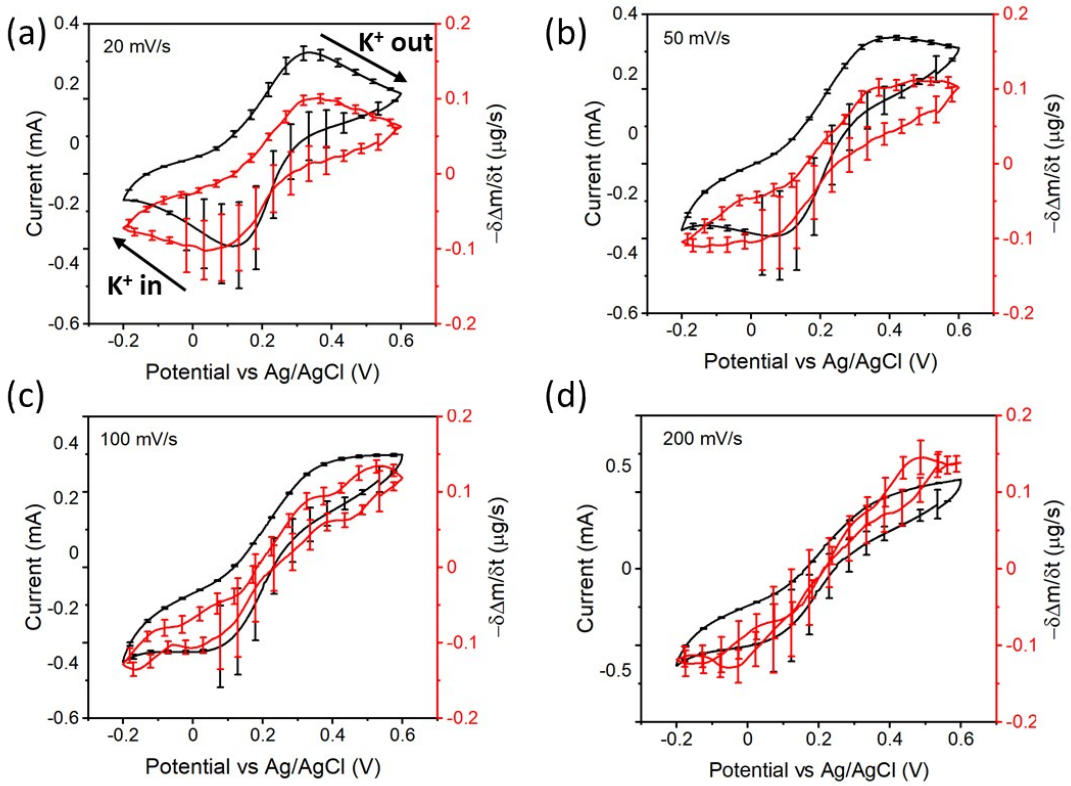

Figure S7 Rate of mass change (from EQCM) vs. potential overlaid with CVs of a Prussian blue thin film cycled in 0.5 M K_2SO_4 for a) 20 mV/s, b) 50 mV/s, c) 100 mV/s, and d) 200 mV/s. The results highlight the close coupling between rate of mass change and electrochemical current in the insertion-type storage mechanism in Prussian blue. Error bars indicate the standard deviation for 10 cycles.

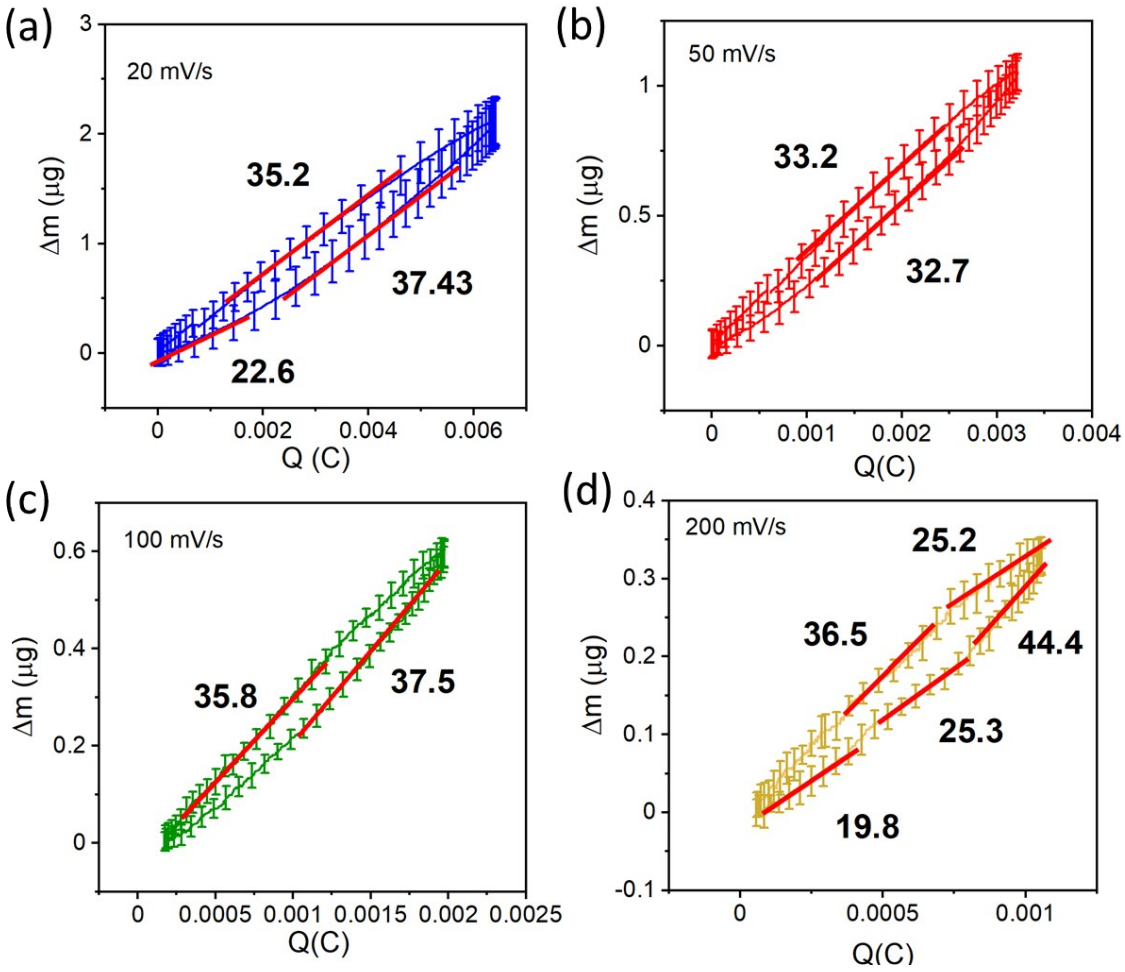

Figure S8 Determination of the mass-to-charge ratio (*m*/*Q*) from EQCM measurement of a Prussian blue thin film cycled in 0.5 M K_2SO_4 for (a) 20 mV/s, (b) 50 mV/s, (c) 100 mV/s, and (d) 200 mV/s. The slopes of the linear regions at 20, 50, and 100 mV/s are consistent with the insertion of K^+ without coordinating water molecules. At 200 mV/s, multiple linear regions are present likely due to the significant polarization of the electrode. Error bars indicate the standard deviation of the mass change at specific charges for 10 cycles.

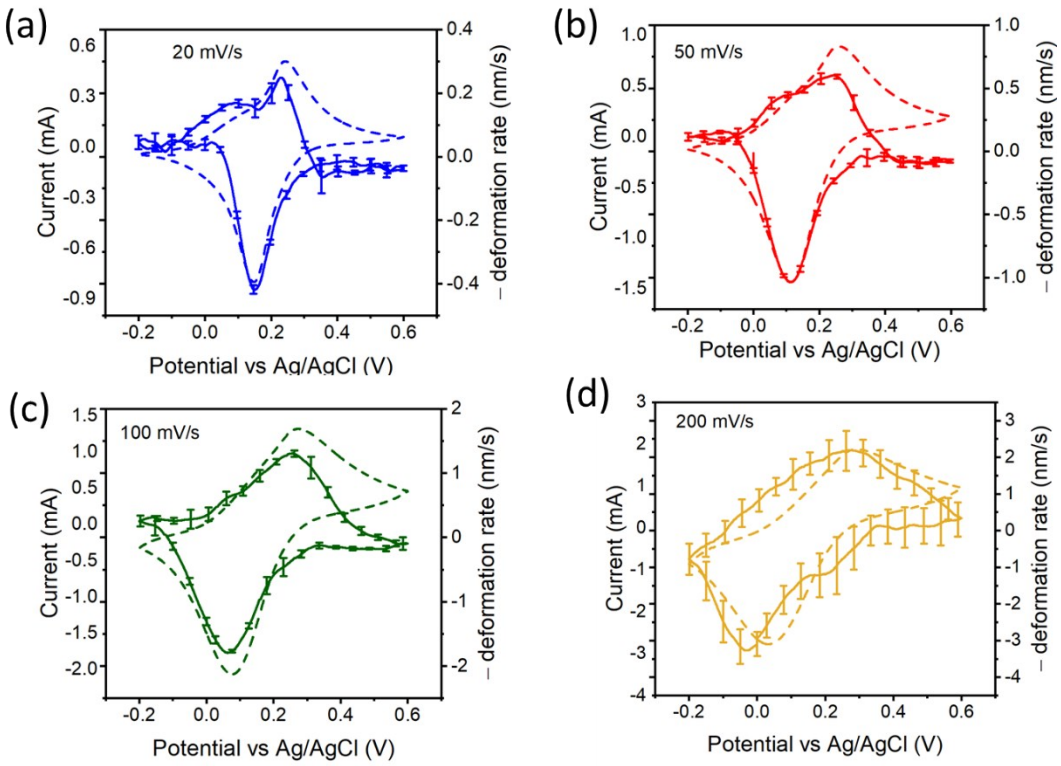

Figure S9 Local *operando* AFM deformation rate vs. potential overlaid with CVs for Prussian blue thin films in 0.5 M K_2SO_4 for a) 20 mV/s, b) 50 mV/s, c) 100 mV/s, and d) 200 mV/s. The results highlight the close coupling between mechanical deformation rate (dashed lines) and electrochemical current (solid lines), as expected for insertion-type electrodes.

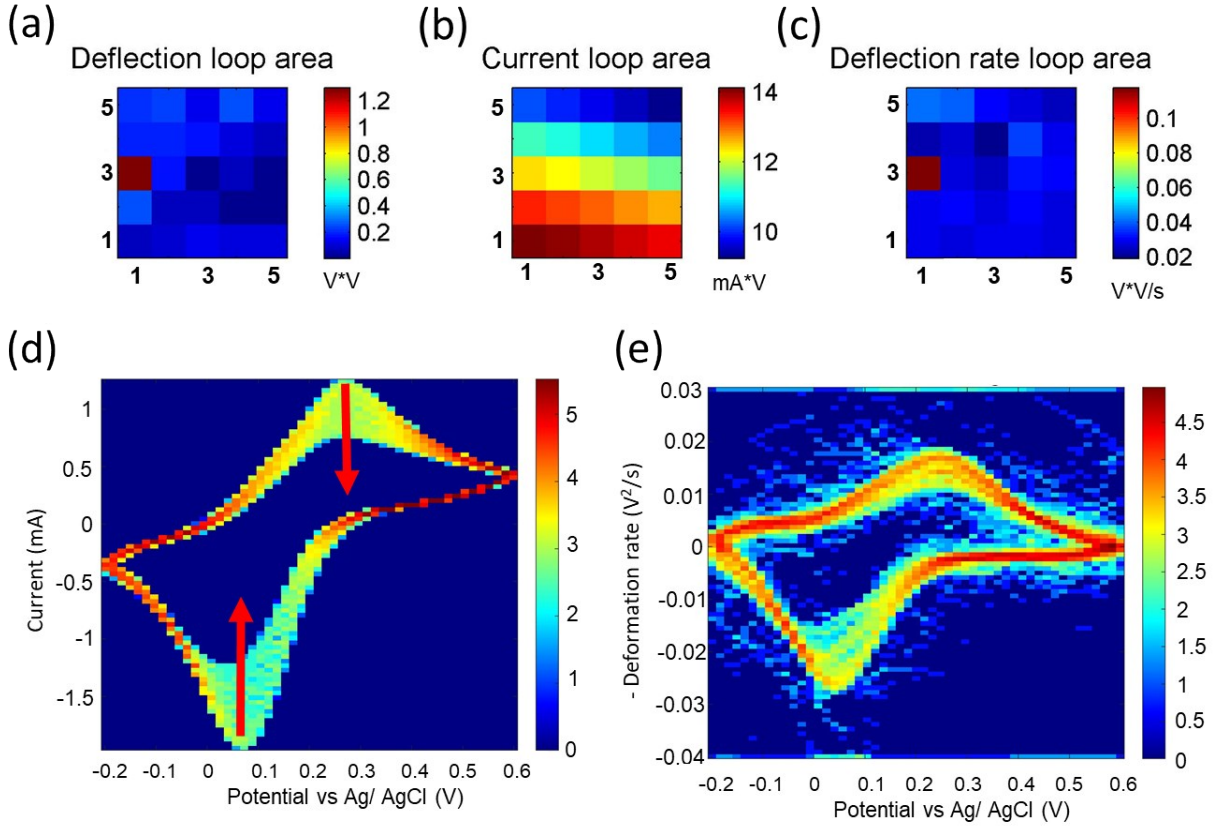

Figure S10 *Operando* AFM map of the heterogeneity of the electrochemically-induced deformation of Prussian blue via a 5 x 5 grid showing loop areas of a) deflection (deformation), b) current, and c) deflection rate. (d) 2D histogram CVs of global current of Prussian blue at 100 mV/s for 500 cycles. (e) 2D histogram of the local deformation rate of Prussian blue at 100 mV/s. These results show there is some degradation of the film occurring over the course of electrochemical cycling in the K_2SO_4 electrolyte, but not as severe as in Li_2SO_4 and Na_2SO_4. (scale bar denotes the logarithm of the cycle count, where red regions indicate the most frequent cycle response; red arrows indicate direction of peak current change during cycling)

References

1 J. J. García-Jareño, D. Benito, J. Navarro-Laboulais and F. Vicente, *J. Chem. Educ.*, 1998, **75**, 881–884.

2 S. R. Systems, 2018, vol. 5.

3 C. Gabrielli, *J. Electrochem. Soc.*, 1991, **138**, 2657.

4 R. Wang, J. B. Mitchell, Q. Gao, W. Tsai, S. Boyd, M. Pharr, N. Balke and V. Augustyn, *ACS Nano*, 2018, **12**, 6032–6039.

5 S. F. A. Kettle, E. Diana, E. M. C. Marchese, E. Boccaleri and P. L. Stanghellini, *J. Raman Spectrosc.*, 2011, **42**, 2006–2014.

6 G. Moretti and C. Gervais, *J Raman Spectrosc*, 2018, **49**, 1198–1204.

7 L. Samain, F. Grandjean, G. J. Long, P. Martinetto, P. Bordet and D. Strivay, *J. Phys. Chem. C*, 2013, **117**, 9693–9712.

8 R. D. Shannon, *Acta Cryst*, 1976, **32**, 751–767.

9 D. A. Sverjensky, *Geochim. Cosmochim. Acta*, 2001, **65**, 3643–3655.

10 Y. Marcus, *Biophys. Chem.*, 1994, **51**, 111–127.